# A Comparative Study of Synchrony Measures for the Early Detection of Alzheimer's Disease Based on EEG

Justin Dauwels, François Vialatte, and Andrzej Cichocki

RIKEN Brain Science Institute, Saitama, Japan
justin@dauwels.com
{fvialatte,cia}@brain.riken.jp

**Abstract.** It has repeatedly been reported in the medical literature that the EEG signals of Alzheimer's disease (AD) patients are less synchronous than in age-matched control patients. This phenomenon, however, does at present not allow to reliably predict AD at an early stage, so-called mild cognitive impairment (MCI), due to the large variability among patients. In recent years, many novel techniques to quantify EEG synchrony have been developed; some of them are believed to be more sensitive to abnormalities in EEG synchrony than traditional measures such as the cross-correlation coefficient. In this paper, a wide variety of synchrony measures is investigated in the context of AD detection, including the cross-correlation coefficient, the mean-square and phase coherence function, Granger causality, the recently proposed correntropy coefficient and two novel extensions, phase synchrony indices derived from the Hilbert transform and time-frequency maps, information-theoretic divergence measures in time domain and time-frequency domain, state space based measures (in particular, non-linear interdependence measures and the S-estimator), and at last, the recently proposed stochastic-event synchrony measures. For the data set at hand, only two synchrony measures are able to convincingly distinguish MCI patients from age-matched control patients ($p < 0.005$), i.e., Granger causality (in particular, full-frequency directed transfer function) and stochastic event synchrony (in particular, the fraction of non-coincident activity). Combining those two measures with additional features may eventually yield a reliable diagnostic tool for MCI and AD.

## 1 Introduction

Many studies have shown that the EEG signals of AD patients are generally less coherent than in age-matched control patients (see [1] for an in-depth review). It is noteworthy, however, that this effect is not always easily detectable: there tends to be a large variability among AD patients. This is especially the case for patients in the pre-symptomatic phase, commonly referred to as Mild Cognitive Impairment (MCI), during which neuronal degeneration is occurring prior to the clinical symptoms appearance. On the other hand, it is crucial to predict AD at an *early* stage: medication that aims at delaying the effects of AD (and hence intend to improve the quality of life of AD patients) are the most effective if applied in the pre-symptomatic phase.

In recent years, a large variety of measures has been proposed to quantify EEG synchrony (we refer to [2]–[5] for recent reviews on EEG synchrony measures); some of those measures are believed to be more sensitive to perturbations in EEG synchrony than classical indices as for example the cross-correlation coefficient or the coherence function. In this paper, we systematically investigate the state-of-the-art of measuring EEG synchrony with special focus on the detection of AD in its early stages. (A related study has been presented in [6, 7] in the context of epilepsy.) We consider various synchrony measures, stemming from a wide spectrum of disciplines, such as physics, information theory, statistics, and

signal processing. Our aim is to investigate which measures are the most suitable for detecting the effect of synchrony perturbations in MCI and AD patients; we also wish to better understand which aspects of synchrony are captured by the different measures, and how the measures are related to each other.

This paper is structured as follows. In Section 2 we review the synchrony measures considered in this paper. In Section 3 those measures are applied to EEG data, in particular, for the purpose of detecting MCI; we describe the EEG data set, elaborate on various implementation issues, and present our results. At the end of the paper, we briefly relate our results to earlier work, and speculate about the neurophysiological interpretation of our results.

## 2 Synchrony Measures

We briefly review the various families of synchrony measures investigated in this paper: cross-correlation coefficient and analogues in frequency and time-frequency domain, Granger causality, phase synchrony, state space based synchrony, information theoretic interdependence measures, and at last, stochastic-event synchrony measures, which we developed in recent work.

### 2.1 Cross-Correlation Coefficient

The cross-correlation coefficient $r$ is perhaps one of the most well-known measures for (linear) interdependence between two signals $x$ and $y$. If $x$ and $y$ are not linearly correlated, $r$ is close to zero; on the other hand, if both signals are identical, then $r = 1$ [8].

### 2.2 Coherence

The coherence function quantifies linear correlations in frequency domain. One distinguishes the magnitude square coherence function $c(f)$ and the phase coherence function $\phi(f)$ [8].

### 2.3 Corr-Entropy Coefficient

The corr-entropy coefficient $r_E$ is a recently proposed [9] non-linear extension of the correlation coefficient $r$; it is close to zero if $x$ and $y$ are independent (which is stronger than being uncorrelated).

### 2.4 Coh-Entropy and Wav-Entropy Coefficient

One can define a non-linear magnitude square coherence function, which we will refer to as "coh-entropy" coefficient $c_E(f)$; it is an extension of the corr-entropy coefficient to the frequency domain. The corr-entropy coefficient $r_E$ can also be extended to the time-frequency domain, by replacing the signals $x$ and $y$ in the definition of $r_E$ by their time-frequency ("wavelet") transforms. In this paper, we use the complex Morlet wavelet, which is known to be well-suited for EEG signals [10]. The resulting measure is called "wav-entropy" coefficient $w_E(f)$. (To our knowledge, both $c_E(f)$ and $w_E(f)$ are novel.)

### 2.5 Granger Causality

Granger causality[1] refers to a family of synchrony measures that are derived from *linear* stochastic models of time series; as the above linear interdependence

[1] The Granger causality measures we consider here are implemented in the BioSig library, available from `http://biosig.sourceforge.net/`.

measures, they quantify to which extent different signals are linearly interdependent. Whereas the above linear interdependence measures are bivariate, i.e., they can only be applied to pairs of signals, Granger causality measures are multivariate, they can be applied to multiple signals *simultaneously*.

Suppose that we are given $n$ signals $X_1(k), X_2(k), \ldots, X_n(k)$, each stemming from a different channel. We consider the multivariate autoregressive (MVAR) model:

$$X(k) = \sum_{\ell=1}^{p} \mathbf{A}(j) X(k-\ell) + E(k), \tag{1}$$

where $X(k) \triangleq (X_1(k), X_2(k), \ldots, X_n(k))^T$, $p$ is the model order, the model coefficients $\mathbf{A}(j)$ are $n \times n$ matrices, and $E(k)$ is a zero-mean Gaussian random vector of size $n$. In words: Each signal $X_i(k)$ is assumed to linearly depend on its own $p$ past values and the $p$ past values of the other signals $X_j(k)$. The deviation between $X(k)$ and this linear dependence is modeled by the noise component $E(k)$. Model (1) can also be cast in the form:

$$E(k) = \sum_{\ell=0}^{p} \tilde{\mathbf{A}}(j) X(k-\ell), \tag{2}$$

where $\tilde{\mathbf{A}}(0) = \mathbf{I}$ (identity matrix) and $\tilde{\mathbf{A}}(j) \triangleq -\mathbf{A}(j)$ for $j > 0$. One can transform (2) into the frequency domain (by applying the $z$-transform and by substituting $z \triangleq e^{-2\pi i \Delta t}$, where $1/\Delta t$ is the sampling rate):

$$X(f) = \tilde{\mathbf{A}}^{-1}(f) E(f) \triangleq \mathbf{H}(f) E(f). \tag{3}$$

The power spectrum matrix of the signal $X(k)$ is determined as

$$\mathbf{S}(f) \triangleq X(f) X(f)^* = \mathbf{H}(f) \mathbf{V} \mathbf{H}^*(f), \tag{4}$$

where $\mathbf{V}$ stands for the covariance matrix of $E(k)$. The Granger causality measures are defined in terms of coefficients of the matrices $\mathbf{A}$, $\mathbf{H}$, and $\mathbf{S}$. Due to space limitations, only a short description of these methods is provided here, additional information can be found in existing literature (e.g., [4]).

From these coefficients, two symmetric measures can be defined:

- Granger coherence $|K_{ij}(f)| \in [0, 1]$ describes the amount of in-phase components in signals $i$ and $j$ at the frequency $f$.
- Partial coherence (PC) $|C_{ij}(f)| \in [0, 1]$ describes the amount of in-phase components in signals $i$ and $j$ at the frequency $f$ when the influence (i.e., linear dependence) of the other signals is statistically removed.

The following asymmetric ("directed") Granger causality measures capture causal relations:

- Directed transfer function (DTF) $\gamma_{ij}^2(f)$ quantifies the fraction of inflow to channel $i$ stemming from channel $j$.
- Full frequency directed transfer function (ffDTF)

$$F_{ij}^2(f) \triangleq \frac{|H_{ij}(f)|^2}{\sum_f \sum_{j=1}^{m} |H_{ij}(f)|^2} \in [0, 1], \tag{5}$$

  is a variation of $\gamma_{ij}^2(f)$ with a global normalization in frequency.
- Partial directed coherence (PDC) $|P_{ij}(f)| \in [0, 1]$ represents the fraction of outflow from channel $j$ to channel $i$
- Direct directed transfer function (dDTF) $\chi_{ij}^2(f) \triangleq F_{ij}^2(f) C_{ij}^2(f)$ is non-zero if the connection between channel $i$ and $j$ is causal (non-zero $F_{ij}^2(f)$) and direct (non-zero $C_{ij}^2(f)$).

### 2.6 Phase Synchrony

Phase synchrony refers to the interdependence between the instantaneous phases $\phi_x$ and $\phi_y$ of two signals $x$ and $y$; the instantaneous phases may be strongly synchronized even when the amplitudes of $x$ and $y$ are statistically independent. The instantaneous phase $\phi_x$ of a signal $x$ may be extracted as [11]:

$$\phi_x^H(k) \triangleq \arg\left[x(k) + i\tilde{x}(k)\right], \tag{6}$$

where $\tilde{x}$ is the Hilbert transform of $x$. Alternatively, one can derive the instantaneous phase from the time-frequency transform $X(k, f)$ of $x$:

$$\phi_x^W(k, f) \triangleq \arg[X(k, f)]. \tag{7}$$

The phase $\phi_x^W(k, f)$ depends on the center frequency $f$ of the applied wavelet. By appropriately scaling the wavelet, the instantaneous phase may be computed in the frequency range of interest.

The phase synchrony index $\gamma$ for two instantaneous phases $\phi_x$ and $\phi_y$ is defined as [11]:

$$\gamma = \left|\left\langle e^{i(n\phi_x - m\phi_y)}\right\rangle\right| \in [0, 1], \tag{8}$$

where $n$ and $m$ are integers (usually $n = 1 = m$). We will use the notation $\gamma_H$ and $\gamma_W$ to indicate whether the instantaneous phases are computed by the Hilbert transform or time-frequency transform respectively. In this paper, we will consider two additional phase synchrony indices, i.e., the evolution map approach (EMA) and the instantaneous period approach (IPA) [12]. Due to space constraints, we will not describe those measures here, instead we refer the reader to [12][2]; additional information about phase synchrony can be found in [6].

### 2.7 State Space Based Synchrony

State space based synchrony (or "generalized synchronization") evaluates synchrony by analyzing the interdependence between the signals in a state space reconstructed domain (see e.g., [7]). The central hypothesis behind this approach is that the signals at hand are generated by some (unknown) deterministic, potentially high-dimensional, non-linear dynamical system. In order to reconstruct such system from a signal $x$, one considers delay vectors $X(k) = (x(k), x(k-\tau), \ldots, x(k-(m-1)\,\tau))^T$, where $m$ is the embedding dimension and $\tau$ denotes the time lag. If $\tau$ and $m$ are appropriately chosen, and the signals are indeed generated by a deterministic dynamical system (to a good approximation), the delay vectors lie on a smooth manifold ("mapping") in $\mathbb{R}^m$, apart from small stochastic fluctuations.

The S-estimator [13], here denoted by $S_{\text{est}}$, is a state space based measure obtained by applying principal component analysis (PCA) to delay vectors[3]. We also considered three measures of nonlinear interdependence, $S^k$, $H^k$, and $N^k$ (see [6] for details[4]).

### 2.8 Information-Theoretic Measures

Several interdependence measures have been proposed that have their roots in information theory. Mutual Information $I$ is perhaps the most well-known information-theoretic interdependence measure; it quantifies the amount of information the random variable $Y$ contains about random variable $X$ (and vice

[2] Program code is available at `www.agnld.uni-potsdam.de/%7Emros/dircnew.m`
[3] We used the S Toolbox downloadable from `http://aperest.epfl.ch/docs/software.htm`
[4] Software is available from `http://www.vis.caltech.edu/~rodri/software.htm`

versa); it is always positive, and it vanishes when $X$ and $Y$ are statistically independent. Recently, a sophisticated and effective technique to compute mutual information between time series was proposed [14]; we will use that method in this paper[5]. The method of [14] computes mutual information in time-domain; alternatively, this quantity may also be determined in time-frequency domain (denoted by $I_W$), more specifically, from normalized spectrograms [15, 16] (see also [17, 18]).

We will also consider several information-theoretic measures that quantify the *dissimilarity* (or "distance") between two random variables (or signals). In contrast to the previously mentioned measures, those divergence measures vanish if the random variables (or signals) are *identical*; moreover, they are not necessarily symmetric, and therefore, they can not be considered as distance measures in the strict sense. Divergences may be computed in time domain and time-frequency domain; in this paper, we will only compute the divergence measures in time-frequency domain, since the computation in time domain is far more involved. We consider the Kullback-Leibler divergence $K$, the Rényi divergence $D_\alpha$, the Jensen-Shannon divergence $J$, and the Jensen-Rényi divergence $J_\alpha$. Due to space constraints, we will not review those divergence measures here; we refer the interested reader to [15, 16].

### 2.9 Stochastic Event Synchrony (SES)

Stochastic event synchrony, an interdependence measure we developed in earlier work [19], describes the similarity between the time-frequency transforms of two signals $x$ and $y$. As a first step, the time-frequency transform of each signal is approximated as a sum of (half-ellipsoid) basis functions, referred to as "bumps" (see Fig. 1 and [20]). The resulting bump models, representing the most prominent oscillatory activity, are then aligned (see Fig. 2): bumps in one time-frequency map may not be present in the other map ("non-coincident bumps"); other bumps are present in both maps ("coincident bumps"), but appear at slightly different positions on the maps. The black lines in Fig. 2 connect the

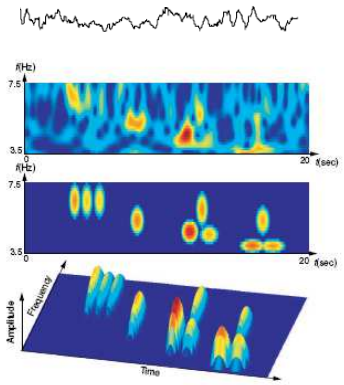


**Fig. 1.** Bump modeling.

centers of coincident bumps, and hence, visualize the offset in position between pairs of coincident bumps. Stochastic event synchrony consists of five parameters that quantify the alignment of two bump models:

- $\rho$: fraction of non-coincident bumps,
- $\delta_t$ and $\delta_f$: average time and frequency offset respectively between coincident bumps,
- $s_t$ and $s_f$: variance of the time and frequency offset respectively between coincident bumps.

[5] The program code (in C) is available at `www.klab.caltech.edu/~kraskov/MILCA/`

The alignment of the two bump models (cf. Fig. 2 (right)) is obtained by iterative max-product message passing on a graphical model; the five SES parameters are determined from the resulting alignment by maximum a posteriori (MAP) estimation [19]. The parameters $\rho$ and $s_t$ are the most relevant for the present study, since they quantify the synchrony between bump models (and hence, the original time-frequency maps); low $\rho$ and $s_t$ implies that the two time-frequency maps at hand are well synchronized.

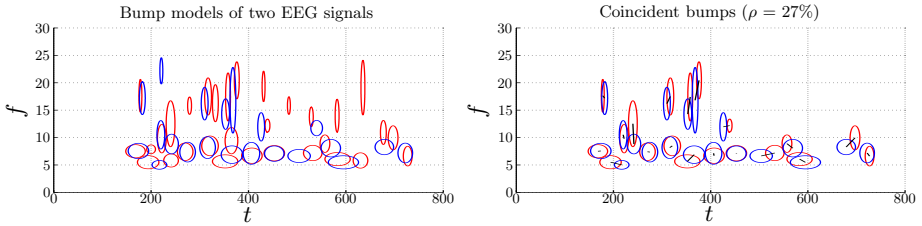


**Fig. 2.** Coincident and non-coincident activity ("bumps"); (left) bump models of two signals; (right) coincident bumps; the black lines connect the centers of coincident bumps.

## 3 Detection of EEG Synchrony Abnormalities in MCI Patients

In the following section, we describe the EEG data we analyzed. In Section 3.2 we address certain technical issues related to the synchrony measures, and in Section 3.3, we present and discuss our results.

### 3.1 EEG Data

The EEG data[6] analyzed here have been analyzed in previous studies concerning early detection of AD [21]–[25]. They consist of rest eyes-closed EEG data recorded from 21 sites on the scalp based on the 10–20 system. The sampling frequency was 200 Hz, and the signals were band pass filtered between 4 and 30Hz. The subjects comprised two study groups. The first consisted of a group of 25 patients who had complained of memory problems. These subjects were then diagnosed as suffering from MCI and subsequently developed mild AD. The criteria for inclusion into the MCI group were a mini mental state exam (MMSE) score above 24, the average score in the MCI group was 26 (SD of 1.8). The other group was a control set consisting of 56 age-matched, healthy subjects who had no memory or other cognitive impairments. The average MMSE of this control group was 28.5 (SD of 1.6). The ages of the two groups were 71.9 $\pm$ 10.2 and 71.7 $\pm$ 8.3, respectively. Pre-selection was conducted to ensure that the data were of a high quality, as determined by the presence of at least 20 sec. of artifact free data. Based on this requirement, the number of subjects in the two groups described above was reduced to 22 MCI patients and 38 control subjects.

### 3.2 Methods

In order to reduce the computational complexity, we aggregated the EEG signals into 5 zones (see Fig. 3); we computed the synchrony measures (except the S-estimator) from the averages of each zone. For all those measures except SES, we used the arithmetic average; in the case of SES, the bump models obtained from the 21 electrodes were clustered into 5 zones by means of the aggregation algorithm described in [20]. We evaluated the S-estimator between each pair of zones by applying PCA to the state space embedded EEG signals of both zones.

We divided the EEG signals in segments of equal length $L$, and computed the synchrony measures by averaging over those segments. Since spontaneous EEG is usually highly non-stationary, and most synchrony measures are strictly speaking only applicable to stationary signals, the length $L$ should be sufficiently

[6] We are grateful to Prof. T. Musha for providing us the EEG data.

small; on the other hand, in order to obtain reliable measures for synchrony, the length should be chosen sufficiently large. Consequently, it is not a priori clear how to choose the length $L$, and therefore, we decided to test several values, i.e., $L = 1$s, 5s, and 20s.

In the case of Granger causality measures, one needs to specify the model order $p$. Similarly, for mutual information (in time domain) and the state space based measures, the embedding dimension $m$ and the time lag $\tau$ needs to be chosen; the phase synchrony indices IPA and EMA involve a time delay $\tau$. Since it is not obvious which parameter values amount to the best performance for detecting AD, we have tried a range of parameter settings, i.e., $p = 1, 2, \ldots, 10$, and $m = 1, 2, \ldots, 10$; the time delay was in each case set to $\tau = 1/30$s, which is the period of the fastest oscillations in the EEG signals at hand.

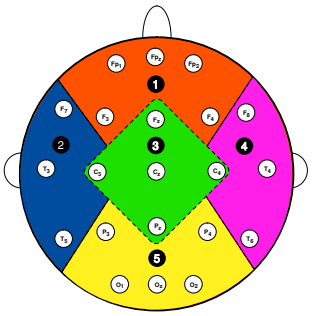


**Fig. 3.** The 21 electrodes used for EEG recording, distributed according to the 10–20 international placement system [8]. The clustering into 5 zones is indicated by the colors and dashed lines (1 = frontal, 2 = left temporal, 3 = central, 4 = right temporal and 5 = occipital).

### 3.3 Results and Discussion

Our main results are summarized in Table 1, which shows the sensitivity of the synchrony measures for detecting MCI. Due to space constraints, the table only shows results for *global* synchrony, i.e., the synchrony measures were averaged over all pairs of zones. (Results for local synchrony and individual frequency bands will be presented in a longer report, including a detailed description of the influence of various parameters such as model order and embedding dimension on the sensitivity.) The p-values, obtained by the Mann-Whitney test, need strictly speaking to be Bonferroni corrected; since we consider many different measures simultaneously, it is likely that a few of those measures have small p-values merely due to stochastic fluctuations (and not due to systematic difference between MCI and control patients). In the most conservative Bonferroni post-correction, the p-values need to be divided by the number of synchrony measures.

From the table, it can be seen that only a few measures evince significant differences in EEG synchrony between MCI and control patients: full-frequency DTF and $\rho$ are the most sensitive (for the data set at hand), their p-values remain significant ($p_{corr} < 0.05$) after Bonferroni correction. In other words, the effect of MCI and AD on EEG synchrony can be detected, as was reported earlier in the literature; we will expand on this issue in the following section.

In other to gain more insight in the relation between the different measures, we calculated the correlation between them (see Fig. 5; red and blue indicate strong correlation and anti-correlation respectively). From this figure, it becomes strikingly clear that the majority of measures are strongly correlated (or anti-correlated) with each other; in other words, the measures can easily be classified in different families. In addition, many measures are strongly (anti-)correlated with the classical cross-correlation coefficient $r$, the most basic measure; as a result, they do not provide much additional information regarding EEG synchrony. Measures that are only weakly correlated with the cross-correlation coefficient include the phase synchrony indices, Granger causality measures, and

stochastic-event synchrony measures; interestingly, those three families of synchrony measures are mutually uncorrelated, and as a consequence, they each seem to capture a specific kind of interdependence.

In Fig. 4, we combine the two most sensitive synchrony measures (for the data set at hand), i.e., full-frequency DTF and $\rho$. In this figure, the MCI patients are fairly well distinguishable from the control patients. As such, the separation is not sufficiently strong to yield reliable early prediction of AD. For this purpose, the two features need to be combined with complementary features, for example, derived from the slowing effect of AD on EEG, or perhaps from different modalities such as PET, MRI, DTI, or biochemical indicators. On the other hand, we remind the reader of the fact that in the data set at hand, patients did not carry out any specific task; moreover, the recordings were short (only 20s). It is plausible that the sensitivity of EEG synchrony could be further improved by increasing the length of the recordings and by recording the EEG before, while, and after patients carry out specific tasks, e.g., working memory tasks.

| Measure | Cross-correlation | Coherence | Phase Coherence | Corr-entropy | Wave-entropy | |
|---|---|---|---|---|---|---|
| p-value | **0.028*** | 0.060 | 0.72 | 0.27 | **0.012*** | |
| References | [8] | | | [9] | | |

| Measure | Granger coherence | Partial Coherence | PDC | DTF | ffDTF | dDTF |
|---|---|---|---|---|---|---|
| p-value | 0.15 | 0.16 | 0.60 | 0.34 | **0.0012**** | **0.030*** |
| References | [4] | | | | | |

| Measure | Kullback-Leibler | Rényi | Jensen-Shannon | Jensen-Rényi | $I_W$ | $I$ |
|---|---|---|---|---|---|---|
| p-value | 0.072 | 0.076 | 0.084 | 0.12 | 0.060 | 0.080 |
| References | [15] | | | | | [14] |

| Measure | $N^k$ | $S^k$ | $H^k$ | S-estimator | | |
|---|---|---|---|---|---|---|
| p-value | **0.032*** | 0.29 | 0.090 | 0.33 | | |
| References | [6] | | | [13] | | |

| Measure | Hilbert Phase | Wavelet Phase | Evolution Map | Instantaneous Period | | |
|---|---|---|---|---|---|---|
| p-value | 0.15 | 0.082 | 0.072 | **0.020*** | | |
| References | [6] | | [12] | | | |

| Measure | $s_t$ | $\rho$ | | | | |
|---|---|---|---|---|---|---|
| p-value | 0.92 | **0.00029**** | | | | |

**Table 1.** Sensitivity of synchrony measures for early prediction of AD (p-values for Mann-Whitney test; * and ** indicate $p < 0.05$ and $p < 0.005$ respectively).

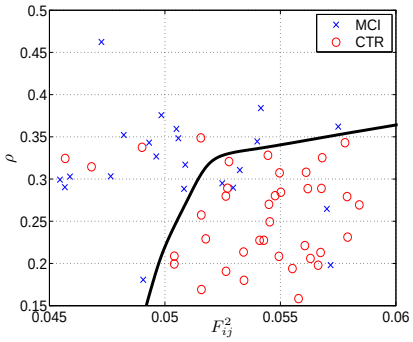


**Fig. 4.** $\rho$ vs. ffDTF

## 4 Conclusions

In previous studies, brain dynamics in AD and MCI patients were mainly investigated using coherence (cf. Section 2.2) or state space based measures of synchrony (cf. Section 2.7). During working memory tasks, coherence shows significant effects in AD and MCI groups [26] [27]; in resting condition, however, coherence does not show such differences in low frequencies (below 30Hz), neither between AD and controls [28] nor between MCI and controls [27]. These results are consistent with our observations. In the gamma range, coherence seems to decrease with AD [29]; we did not investigate this frequency range,

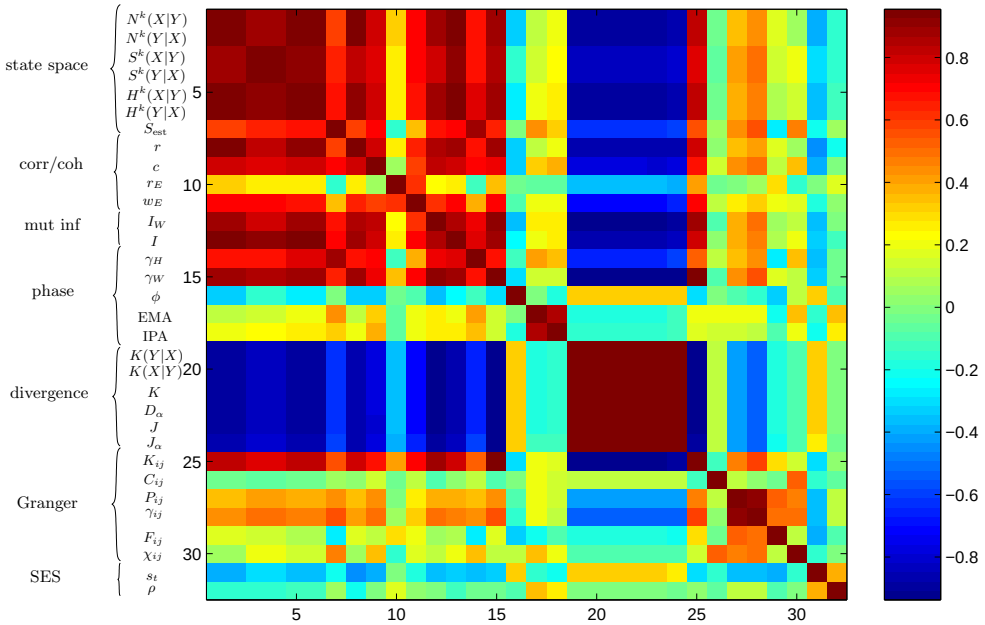


**Fig. 5.** Correlation between the synchrony measures

however, since the EEG signals analyzed here were band pass filtered between 4 and 30Hz.

Synchronization likelihood, a state space based synchronization measure similar to the non-linear interdependence measures $S^k$, $H^k$, and $N^k$ (cf. Section 2.7), is believed to be more sensitive than coherence to detect changes in AD patients [28]. Using state space based synchrony methods, significant differences were found between AD and control in rest conditions [28] [30] [32] [33]. State space based synchrony failed to retrieve significant differences between MCI patient and control subjects on a global level [32] [33], but significant effects were observed *locally*: fronto-parietal electrode synchronization likelihood progressively decreased through MCI and mild AD groups [30]. We report here a lower p-value for the state space based synchrony measure $N^k$ ($p = 0.032$) than for coherence ($p = 0.06$); those low p-values, however, would not be statistically significant after Bonferroni correction.

By means of Global Field Synchronization, a phase synchrony measure similar to the ones we considered in this paper, Koenig et al. [31] observed a general decrease of synchronization in correlation with cognitive decline and AD. In our study, we analyzed five different phase synchrony measures: Hilbert and wavelet based phase synchrony, phase coherence, evolution map approach (EMA), and instantaneous period approach (IPA). The p-value of the latter is low ($p = 0.020$), in agreement with the results of [31], but it would be non-significant after Bonferroni correction.

The strongest observed effect is a significantly higher degree of local asynchronous activity ($\rho$) in MCI patients, more specifically, a high number of non-coincident, asynchronous oscillatory events ($p = 0.00029$). Interestingly, we did not observe a significant effect on the timing jitter $s_t$ of the coincident events ($p = 0.92$). In other words, our results seem to indicate that there is significantly more non-coincident background activity, while the *coincident* activity remains well synchronized. On the one hand, this observation is in agreement with previous studies that report a general decrease of neural synchrony in MCI and AD patients; on the other hand, it goes beyond previous results, since it yields a more subtle description of EEG synchrony in MCI and AD patients: it suggests that the loss of coherence is mostly due to an increase of (local) non-coincident background activity, whereas the locked (coincident) activity remains equally well synchronized. In future work, we will verify this conjecture by means of other data sets.

## References


1. J. Jong, "EEG Dynamics in Patients with Alzheimer's Disease," *Clinical Neurophysiology,* 115:1490–1505 (2004).
2. E. Pereda, R. Q. Quiroga, and J. Bhattacharya, "Nonlinear Multivariate Analysis of Neurophsyiological Signals," *Progress in Neurobiology,* 77 (2005) 1–37.
3. M. Breakspear, "Dynamic Connectivity in Neural Systems: Theoretical and Empirical Considerations," *Neuroinformatics,* vol. 2, no. 2, 2004.
4. M. Kamiński and Hualou Liang, "Causal Influence: Advances in Neurosignal Analysis," *Critical Review in Biomedical Engineering,* 33(4):347–430 (2005).
5. C. J. Stam, "Nonlinear Dynamical Analysis of EEG and MEG: Review of an Emerging Field," *Clinical Neurophysiology* 116:2266–2301 (2005).
6. R. Q. Quiroga, A. Kraskov, T. Kreuz, and P. Grassberger, "Performance of Different Synchronization Measures in Real Data: A Case Study on EEG Signals," *Physical Review E,* vol. 65, 2002.
7. V. Sakkalis, C. D. Giurcăneacu, P. Xanthopoulos, M. Zervakis, V. Tsiaras, Yianghua Yang, and S. Micheloyannis, "Assessment of Linear and Non-Linear EEG Synchronization Measures for Evaluating Mild Epileptic Signal Patterns," *Proc. of ITAB 2006*, Ioannina-Epirus, Greece, October 26–28, 2006.
8. P. Nunez and R. Srinivasan, *Electric Fields of the Brain: The Neurophysics of EEG,* Oxford University Press, 2006.
9. Jian-Wu Xu, H. Bakardjian, A. Cichocki, and J. C. Principe, "EEG Synchronization Measure: a Reproducing Kernel Hilbert Space Approach," submitted to *IEEE Transactions on Biomedical Engineering Letters*, Sept. 2006.
10. C. S. Herrmann, M. Grigutsch, and N. A. Busch, "EEG Oscillations and Wavelet Analysis," in Todd Handy (ed.) *Event-Related Potentials: a Methods Handbook* pp. 229–259, Cambridge, MIT Press, 2005.
11. J.-P. Lachaux, E. Rodriguez, J. Martinerie, and F. J. Varela, "Measuring Phase Synchrony in Brain Signals," *Human Brain Mapping* 8:194–208 (1999).
12. M. G. Rosenblum, L. Cimponeriu, A. Bezerianos, A. Patzak, and R. Mrowka, "Identification of Coupling Direction: Application to Cardiorespiratory Interaction," *Physical Review E,* 65 041909, 2002.
13. C. Carmeli, M. G. Knyazeva, G. M. Innocenti, and O. De Feo, "Assessment of EEG Synchronization Based on State-Space Analysis," *Neuroimage,* 25:339–354 (2005).
14. A. Kraskov, H. Stögbauer, and P. Grassberger, "Estimating Mutual Information," *Phys. Rev. E* 69 (6) 066138, 2004.
15. S. Aviyente, "A Measure of Mutual Information on the Time-Frequency Plane," *Proc. of ICASSP 2005,* vol. 4, pp. 481–484, March 18–23, 2005, Philadelphia, PA, USA.
16. S. Aviyente, "Information-Theoretic Signal Processing on the Time-Frequency Plane and Applications," *Proc. of EUSIPCO 2005,* Sept. 4–8, 2005, Antalya, Turkey.
17. Q. R. Quiroga, O. Rosso, and E. Basar, "Wavelet-Entropy: A Measure of Order in Evoked Potentials," *Electr. Clin. Neurophysiol. (Suppl.)*, 49:298–302 (1999).
18. S. Blanco, R. Q. Quiroga, O. Rosso, and S. Kochen, "Time-Frequency Analysis of EEG Series," *Physical Review E* 51:2624 (1995).
19. J. Dauwels, F. Vialatte, and A. Cichocki, "A Novel Measure for Synchrony and Its Application to Neural Signals," *Proc. IEEE Int. Conf. on Acoustics and Signal Processing (ICASSP),* Honolulu, Hawai'i, USA, April 15–20, 2007.
20. F. Vialatte, C. Martin, R. Dubois, J. Haddad, B. Quenet, R. Gervais, and G. Dreyfus, "A Machine Learning Approach to the Analysis of Time-Frequency Maps, and Its Application to Neural Dynamics," *Neural Networks,* 2007, 20:194–209.
21. R. Chapman et al., "Brain Event-Related Potentials: Diagnosing Early-Stage Alzheimer's Disease," *Neurobiol. Aging* 28:194–201, 2007.
22. A. Cichocki et al., "EEG Filtering Based on Blind Source Separation (BSS) for Early Detection of Alzheimer's Disease," *Clin. Neurophys.* 116:729–37, 2005.
23. M. Hogan et al., "Memory-Related EEG Power and Coherence Reductions in Mild Alzheimer's Disease," *Int. J. Psychophysiol.*, 49, 2003.
24. T. Musha et al., "A New EEG Method for Estimating Cortical Neuronal Impairment that is Sensitive to Early Stage Alzheimer's Disease," *Clin. Neurophys.* 113:1052–8, 2002.
25. F. Vialatte et al., "Blind Source Separation and Sparse Bump Modelling of Time-Frequency Representation of EEG Signals: New Tools for Early Detection of Alzheimer's Disease," *IEEE Workshop on Machine Learning for Signal Processing,* pp. 27–32, 2005.
26. M. J. Hogan, G. R. Swanwick, J. Kaiser, M. Rowan, and B. Lawlor, "Memory-Related EEG Power and Coherence Reductions in Mild Alzheimer's Disease," *Int J Psychophysiol,* 49(2):147–63 (2003).
27. Z. Y. Jiang, "Study on EEG Power and Coherence in Patients with Mild Cognitive Impairment During Working Memory Task," *J Zhejiang Univ Sci B,* 6(12):1213–9 (2005).
28. C. J. Stam, A. M. van Cappellen van Walsum, Y. A. Pijnenburg, H. W. Berendse, J. C. de Munck, P. Scheltens, B. W. van Dijk, "Generalized Synchronization of MEG Recordings in Alzheimer's Disease: Evidence for Involvement of the Gamma Band," *J Clin Neurophysiol,* 19(6):562–74 (2002).
29. C. S. Herrmann and T. Demiralp, "Human EEG Gamma Oscillations in Neuropsychiatric Disorders," *Clinical Neurophysiology,* 116:2719–2733 (2005).
30. C. Babiloni, R. Ferri, G. Binetti, A. Cassarino, G. D. Forno, M. Ercolani, F. Ferreri, G. B. Frisoni, B. Lanuzza, C. Miniussi, F. Nobili, G. Rodriguez, F. Rundo, C. J. Stam, T. Musha, F. Vecchio, and P. M. Rossini, "Fronto-Parietal Coupling of Brain Rhythms in Mild Cognitive Impairment: A Multicentric EEG Study," *Brain Res Bull,* 69(1):63–73 (2006).
31. T. Koenig, L. Prichep, T. Dierks, D. Hubl, L. O. Wahlund, E. R. John, and V. Jelic, "Decreased EEG Synchronization in Alzheimer's Disease and Mild Cognitive Impairment," *Neurobiol Aging,* 26(2):165–71 (2005).
32. Y. A. Pijnenburg, Y. vd Made, A. M. van Cappellen van Walsum, D. L. Knol, P. Scheltens, C. J. Stam, "EEG Synchronization Likelihood in Mild Cognitive Impairment and Alzheimer's Disease During a Working Memory Task," *Clin Neurophysiol,* 115(6):1332–9 (2004).
33. T. Yagyu, J. Wackermann, M. Shigeta, V. Jelic, T. Kinoshita, K. Kochi, P. Julin, O. Almkvist, L. O. Wahlund, I. Kondakor, D. Lehmann, "Global dimensional complexity of multichannel EEG in mild Alzheimer's disease and age-matched cohorts," *Dement Geriatr Cogn Disord,* 8(6):343–7 (1997).